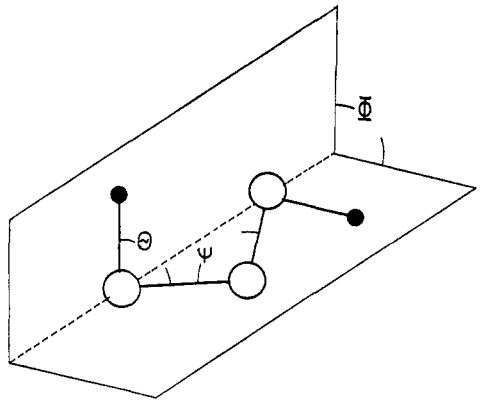

Figure 1. Skew chain structural model of H_2O_3.

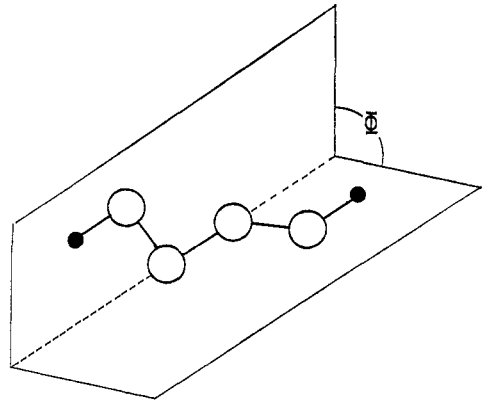

Figure 2. Skew chain structural model of H_2O_4 with dihedral angle between two OOH groups.

lowest theoretical energy for each molecule was used to calculate the energy of reaction 1. In spite of the

$$H_2O_3 \begin{cases} \longrightarrow H_2O + O_2{}^1\Delta_g & E_a = 0.03859 \text{ au} \\ \longrightarrow H_2O_2 + \tfrac{1}{2}O_2{}^1\Delta_g & E_b = 0.02745 \text{ au} \end{cases} \quad (1)$$

fact that complete geometrical optimization was not made it can be seen that the energy difference ($E_a - E_b$) between the two decomposition reactions is rather small. Different experimental conditions may favor one or the other.

The energy of the decomposition reaction of H_2O_4 (reaction 2) indicates that this compound is a stable

$$H_2O_4 \longrightarrow H_2O_2 + O_2{}^1\Delta_g \qquad E = 0.05034 \text{ au} \quad (2)$$

molecular species with respect to decomposition into oxygen and hydrogen peroxide.

Although no calculations were made on organic polyoxides, we believe that the geometry of these compounds should be similar to that reported here. Namely, it was found that steric influence of substituents on stereochemistry of organic peroxides is very small at the interatomic distances and angles being considered.[11]

Acknowledgment. The authors are deeply indebted to Professor J. A. Pople for his permission to use the program written by him and coworkers and especially to Dr. W. J. Hehre for the CDC version of it. This work was supported by the Boris Kidrič Fund.

(11) M. Sax and R. K. McMullan, *Acta Crystallogr.*, **22**, 281 (1967).

Effect of Molecular Geometry on Spin–Orbit Coupling of Aromatic Amines in Solution. Diphenylamine, Iminobibenzyl, Acridan, and Carbazole[1a]

J. Elaine Adams, W. W. Mantulin, and J. Robert Huber* [1b]

Contribution from the Photochemistry and Spectroscopy Laboratory, Department of Chemistry, Northeastern University, Boston, Massachusetts 02215.
Received January 2, 1973

Abstract: The fluorescence quantum yield, the phosphorescence quantum yield, and the lifetimes of a series of aromatic amines (diphenylamine, iminobibenzyl, acridan, and carbazole), whose molecular configurations gradually change from a distinctly nonplanar to a planar geometry, have been investigated at 298 and 77°K in EPA solution. From these data, the important deactivation parameters of the excited states have been derived. The intersystem crossing rate constants and the radiative phosphorescence rate constants decrease dramatically in going from diphenylamine to carbazole, while the radiative fluorescence rate constants change only slightly, leading to the conclusion that the excited state behavior of aromatic amines is dominated by the influence of molecular geometry on spin–orbit coupling.

Spin–orbit coupling in aromatic amines is enhanced relative to aromatic hydrocarbons, as evidenced by increased phosphorescence to fluorescence quantum yield ratios and shorter phosphorescence lifetimes.[2]

These properties of aromatic amines are intermediate between those expected for aza-nitrogen heterocyclics with lowest $n\pi^*$ and lowest $\pi\pi^*$ triplet states.[3] It was

(1) (a) Presented at the 163rd National Meeting of the American Chemical Society, Boston, Mass., April 9–14, 1972. (b) Author to whom correspondence should be addressed at the Fachbereich Chemie, Universität Konstanz, Konstanz, Germany.

(2) V. L. Ermolaev, *Opt. Spektrosk.*, **11**, 492 (1961); *Opt. Spektrosc. (USSR)*, **11**, 266 (1961).

(3) S. P. McGlynn, T. Azumi, and M. Kinoshita, "Molecular Spectroscopy of the Triple State," Prentice-Hall, Englewood Cliffs, N. J., 1969, p 247.

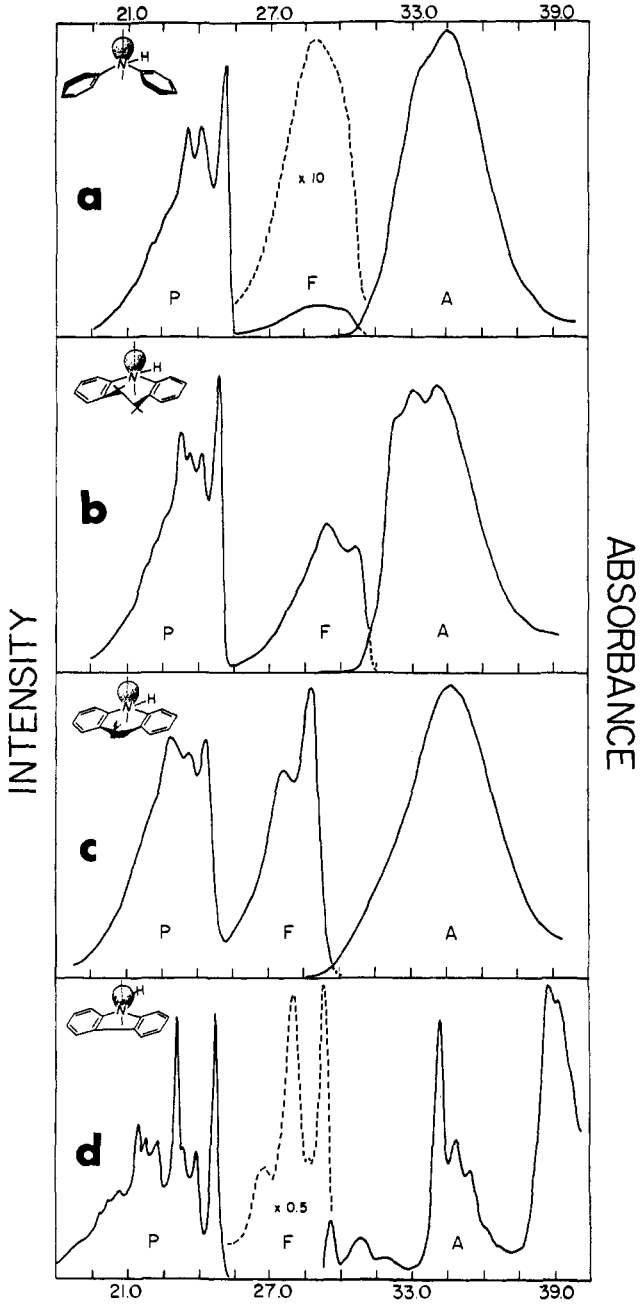

Figure 1. Absorption (A), fluorescence (F), and phosphorescence (P) spectra of (a) diphenylamine, (b) iminobibenzyl, (c) acridan, and (d) carbazole in EPA at 77°K.

suggested by two research groups[4,5] that the effective intersystem crossing in aromatic amines such as aniline is attributable to the pseudo-nonbonding character of the nitrogen lone pair electrons. Lim and Chakrabarti[4] presented theoretical and experimental results which indicate that intramolecular charge-transfer transitions, resulting from the presence of the lone pair electrons, play an important role in spin–orbit coupling. Kasha and Rawls[5] reported experimental evidence to support their formulation of the singlet–triplet transition probability as a function of the angle of twist of the lone pair orbital with respect to the neighboring π orbitals.

In a recently published paper[6] we reported the results of an emission study of phenoxazine and suggested that a change in excited state geometry from the planar ground state could be responsible for its very effective spin–orbit coupling. The geometry at the nitrogen atom is directly related to the way in which the lone pair orbital participates in the electronic structure of the molecule.

Two general classes of transitions appear to be important in the near ultraviolet spectra of aromatic amines. One consists of the $\pi\pi^*$ transitions among nonlocalized molecular orbitals which largely involve the π system of the hydrocarbon moiety. The second class is the charge-transfer transitions, designated $l \rightarrow a_\pi$ by Kasha,[7] in which an electron from the lone pair orbital is promoted to one of the antibonding orbitals of the π system. The lone pair orbital may significantly perturb the $\pi\pi^*$ transitions through conjugation, but this requires certain spatial consideration for an effective overlap between the lone pair orbital and the aromatic π system. In the study of a series of substituted *N,N*-dimethylanilines by Murrell,[8] the oscillator strengths for transitions with substantial charge-transfer character seemed to be particularly sensitive to molecular geometry.

In order to study the influence of the geometry of the lone pair orbital on spin–orbit coupling, we have examined the absorption and emission properties for a series of aromatic amines: diphenylamine (DPA), iminobibenzyl (IBB), acridan (AC), and carbazole (C) (*cf.* Figure 1). The π systems for all these molecules are isoelectronic with diphenylamine, but increasing intramolecular constraint through the introduction of chemical bonds between the phenyl rings forces the molecule into increasingly planar configurations. With this series we avoid the complication of separating geometry effects from phenylation effects such as exciton splitting, as would be the case in comparing aniline, diphenylamine, and triphenylamine. Secondly, we avoid the assessment of substituent inductive effects, as the comparison of aniline with its methyl and ethyl N-substituted analogs would necessitate. Alkyl substitution on the benzene ring does not appear to perturb the near-ultraviolet absorption spectrum in a significant manner.[9] Thirdly, this series is appropriate for study because it more closely resembles larger aromatic amine systems present in biological and pharmacological molecules than do simpler amine systems.

We have determined the emission quantum yields and measured lifetimes in solution at room temperature and at 77°K for the aromatic amines mentioned above. From these data we have obtained the intersystem crossing rate constants and natural phosphorescence lifetimes, the parameters which indicate directly the degree of spin–orbit coupling between the singlet and triplet manifolds. The results of our study clearly demonstrate the importance of molecular geometry on the behavior of the excited states of aromatic amines.

Experimental Section

Materials. Diphenylamine (zone refined), acridan, iminobi-

(4) E. C. Lim and S. K. Chakrabarti, *Chem. Phys. Lett.*, **1**, 28 (1967); *J. Chem. Phys.*, **47**, 4726 (1967).
(5) M. Kasha and H. R. Rawls, *Photochem. Photobiol.*, **7**, 561 (1968).
(6) J. R. Huber and W. W. Mantulin, *J. Amer. Chem. Soc.*, **94**, 3755 (1972).
(7) M. Kasha, "Light and Life," W. D. McElroy and B. Glass, Ed., Johns Hopkins University Press, Baltimore, Md., 1961, p 31.
(8) J. N. Murrell, *J. Chem. Soc.*, 3779 (1956).
(9) H. B. Klevens and J. R. Platt, *J. Amer. Chem. Soc.*, **71**, 1714 (1949).

Table I. Absorption Frequencies and Oscillator Strengths in EPA

Molecule	$\Delta E(S_1-S_0)$ (77°K),[a] cm^{-1}	$\Delta E(S_2-S_0)$ (77°K),[b] cm^{-1}	f_{tot} 298°K	f_{tot} 77°K	$f^0(S_1-S_0)$[c] 298°K	$f^0(S_1-S_0)$[c] 77°K	$f(S_2-S_0)$ (77°K)
DPA	31,100	34,400	0.43	0.51	0.072	0.068	0.44[d]
IBB	31,100	34,100	0.41	0.45	0.072	0.072	0.38[d]
AC	29,700	34,600	0.31	0.32	0.054	0.055	0.27[d]
C	29,500	34,030	0.049		0.054	0.053	0.15

[a] Absorption-fluorescence crosspoint. [b] Absorption maximum. [c] Calculated: $f^0(S_1-S_0) = 1.5\bar{\nu}^{-2}k_f^0$. For k_f^0 see Table II. [d] Calculated: $f(S_2-S_0) = f_{tot} - f^0(S_1-S_0)$.

benzyl, and carbazole (zone refined) (Aldrich Chemical Co.) were purified by repeated recrystallization from aqueous ethanol or petroleum ether (bp 60–100°). The final recrystallization occurred under a nitrogen atmosphere. EPA (diethyl ether, isopentane, ethanol, 5:5:2; American Instrument Co.) was used as received. Ethanol required no further purification.

Apparatus and Procedure. The absorption measurements were performed with a Cary 14 spectrophotometer. The spectrophotofluorimeter employed in this study consists of a 450-W xenon arc excitation source, a Bausch and Lomb fl 500 mm, *f*/4.4 monochromator, and a Spex fl 750 mm, *f*/6.8 analyzing monochromator. A more detailed description of this apparatus is presented elsewhere.[10]

The absorption and emission spectra are plotted by computer and the latter are corrected for the response characteristics of the instrument. Provision is made for temperature control of the samples from room temperature to 77°K using a quartz dewar vessel equipped with a copper block sample compartment.[11] The samples (solute concentration $<5 \times 10^{-5}$ *M*) were prepared in quartz cells; the solutions were deoxygenated either by repeated freeze-pump-thaw cycles or by passing nitrogen gas through the solution for several minutes.

The quantum yields at room temperature were determined relative to the quantum yields of both quinine bisulfate in aqueous 0.1 *N* sulfuric acid ($\phi_f = 0.55$),[12,13] and anthracene in ethanol ($\phi_f = 0.28$).[12,14] Corrections were made for differences between the index of refraction of the reference and sample solutions. The quantum yields at intervals between room temperature and 77°K were established relative to the room temperature quantum yields with corrections for changes in solute concentration, index of refraction, and absorptivity with temperature. A detailed description of this procedure is presented elsewhere.[15]

The fluorescence lifetimes were measured by the single photon counting technique.[16] The apparatus employed utilized a nanosecond flash lamp filled with 37 cm of deuterium gas. The decay curves were analyzed by a deconvolution procedure.

Phosphorescence lifetimes were determined with the spectrophotofluorimeter by blocking the excitation light beam with a simple camera shutter and recording the decay signal on an oscilloscope.

Results

Absorption Spectra. The absorption spectra of DPA, IBB, AC, and C in EPA at 77°K are presented in Figure 1; data pertaining to these spectra are collected in Table I. The extinction coefficients at the wavelengths of maximum absorbance are in agreement with those reported by Itier and Casadevall.[17] Oscillator strengths *f* at 77°K were obtained by comparison with those at room temperature, with corrections for changes in solute concentration due to increases in solvent density. Included in Table I are also the oscillator strengths f^0 calculated from natural fluorescence lifetimes using the relationship[18] $f^0 = 1.5/(\bar{\nu}^2\tau_f^0)$, where τ_f^0 and $\bar{\nu}$ are the natural fluorescence lifetime and the absorption–fluorescence crosspoint in reciprocal centimeters, respectively.

Emission Spectra. The emission spectra of DPA, AC, and C, shown in Figure 1, are in agreement with previously published data.[2,19,20] In all cases the phosphorescence exhibits sharper vibrational structure than the fluorescence. The 0–0 transition is prominent in the phosphorescence and several vibrational progressions can be observed, particularly in C. The fluorescence becomes more structured in going from DPA to C.

Emission Quantum Yields and Lifetimes. Data pertaining to the fluorescence quantum yields ϕ_f, phosphorescence quantum yields ϕ_p, and lifetimes in EPA are collected in Tables II and III. Bowen and Eland[21] reported the fluorescence quantum yield for DPA to be about 0.05 in deoxygenated solutions of methanol, 2-propanol, and hexane. Berlman,[22] published a value of 0.38 for C in a cyclohexane solution. The room temperature quantum yields we report are averages of 8 to 15 determinations, including comparison with two fluorescence standards at two or three exciting wavelengths.

The fluorescence quantum yields of IBB and AC increase at lower temperatures, while those of DPA and C remain relatively unchanged. The phosphorescence lifetimes $\tau_p = 1/k_p$ measured by Ermolaev[2] and Rawls[23] are in good agreement with our values, but the quantum yield ratios ϕ_p/ϕ_f we report are consistently about 10% smaller than those of Ermolaev. Since the fluorescence of the aromatic amines in ethanolic solutions exhibit a long wavelength tail which extends well into the phosphorescence region, this tail portion was taken into account in the calculation of our quantum yield ratios. We presume the spectral shape of the fluorescence at 77°K is identical with that near 100°K where no phosphorescence is present.

Discussion

The lowest energy absorption bands of DPA, IBB, and AC are similar in appearance (*cf.* Figure 1). Absorbance originates near 30,000 cm^{-1} and maximizes near 34,000 cm^{-1}; the bands are intense, and any structural features which appear at lower temperatures are

(10) H. J. Pownall and J. R. Huber, *J. Amer. Chem. Soc.*, **93**, 6429 (1971).
(11) E. Fischer, *J. Mol. Photochem.*, **2**, 99 (1968).
(12) C. A. Parker, "Photoluminescence of Solutions," Elsevier, New York, N. Y., 1968.
(13) W. H. Melhuish, *J. Phys. Chem.*, **65**, 229 (1961).
(14) J. N. Demas and G. A. Crosby, *J. Phys. Chem.*, **75**, 991 (1971).
(15) W. W. Mantulin and J. R. Huber, *Photochem. Photobiol.*, **17**, 139 (1973).
(16) W. R. Ware, "Creation and Detection of the Excited State," A. Lamola, Ed., Marcel Dekker, New York, N. Y., 1971.
(17) J. Itier and A. Casadevall, *Bull. Soc. Chim. Fr.*, 168 (1969).
(18) Obtained from information in J. B. Birks, "Photophysics of Aromatic Molecules," Wiley-Interscience, New York, N. Y., 1970, p 88.
(19) V. Zanker and B. Schneider, *Z. Phys. Chem. (Frankfurt am Main)*, **68**, 19 (1969).
(20) N. Mataga, Y. Torishahi, and K. Ezumi, *Theor. Chim. Acta*, **2**, 158 (1964).
(21) E. J. Bowen and H. H. D. Eland, *Chem. Soc. Proc.*, 202 (1963).
(22) I. B. Berlman, "Handbook of Fluorescence Spectra of Aromatic Molecules," Academic Press, New York, N. Y., 1971, p 207.
(23) H. R. Rawls, Doctoral Thesis, Florida State University, 1964.

Table II. Fluorescence Quantum Yields, Fluorescence Rate Constants, Intersystem Crossing Rate Constants in EPA at 298 and 77°K

Molecule	ϕ_f 298°K	ϕ_f 77°K	k_f,[a,d] 10^7 sec^{-1} 298°K	k_f,[a,d] 10^7 sec^{-1} 77°K	k_f^0,[b] 10^7 sec^{-1} 298°K	k_f^0,[b] 10^7 sec^{-1} 77°K	k_{isc}(77°K),[c] 10^7 sec^{-1}
DPA	0.11 ± 0.1	0.11 ± 0.01	42	40	4.6	4.4	36
IBB	0.24 ± 0.03	0.32 ± 0.04	19	14	4.5	4.5	10
AC	0.32 ± 0.03	0.38 ± 0.05	9.6	8.4	3.1	3.2	5.2
C	0.42 ± 0.04	0.44 ± 0.04	6.5	6.7	2.7	3.0	3.7

[a] $k_f = 1/\tau_f$. [b] $k_f^0 = \phi_f/\tau_f$. [c] $k_{isc} = k_f - k_f^0$. [d] Estimated error <10%.

Table III. Phosphorescence Quantum Yields, Phosphorescence Rate Constants, Nonradiative Rate Constants in EPA at 77°K

Molecule	$\Delta E(T_1-S_0)$, cm^{-1}	$\Delta E(S_1-T_1)$, cm^{-1}	ϕ_p/ϕ_f	ϕ_p[a]	q_p[b]	k_p,[c] sec^{-1}	k_p^0,[d] sec^{-1}	k_{nr},[e] sec^{-1}
DPA	25,140	5960	6.65 ± 0.15	0.73	0.82	0.50 ± 0.05	0.41	0.09
IBB	24,770	6330	1.60 ± 0.06	0.51	0.75	0.36 ± 0.03	0.27	0.09
AC	24,330	5370	1.35 ± 0.07	0.51	0.82	0.29 ± 0.02	0.24	0.05
C	24,690	4810	0.55 ± 0.02	0.24	0.43	0.13 ± 0.01	0.056	0.07

[a] $\phi_f(77°K)(\phi_p/\phi_f) = \phi_p$. [b] $q_p = \phi_p/(1 - \phi_f)$. [c] $k_p = 1/\tau_p$. [d] $k_p^0 = q_p/\tau_p$. [e] $k_{nr} = k_p - k_p^0$.

diffuse. Carbazole, on the other hand, exhibits two absorption bands with sharp vibrational structure in the same energy region: $\Delta E(S_1-S_0) = 29{,}500$ cm^{-1} with $f = 0.049$ and $\Delta E(S_2-S_0) = 34{,}030$ cm^{-1} with $f = 0.15$. The measured oscillator strength (f) for the first electronic transition in C is in good agreement with the oscillator strength (f^0) calculated from the natural fluorescence lifetime, but the measured oscillator strengths of DPA, IBB, and AC are much larger than the calculated values (*cf.* Table I). Since natural fluorescence lifetimes produce reliable oscillator strengths for other aromatic amines (*e.g.*, aniline, $f = 0.028$;[24] $f^0 = 0.033$[25]), we propose that the observed discrepancies indicate that at least *two electronic transitions* lie under the "first absorption band" of DPA, IBB, and AC. Thus, the oscillator strength of the lowest energy transition can be determined from the natural fluorescence lifetime, while that of the second, more intense transition, may be obtained by subtraction of $f^0(S_1-S_0)$ from f_{tot}, the measured oscillator strength of the whole absorption band. The f values for the first and second transition obtained in this fashion are also listed in Table I. Additional experimental findings also indicate that the broad, longest wavelength absorption band consists of more than one, and most probably two, electronic transitions. Thus, the fluorescence spectra of DPA, IBB, and AC are not mirror images of their respective absorption bands; the half-width of the absorption is 1000 to 2000 cm^{-1} larger than the fluorescence half-width. Moreover, the relative excitation polarization, monitored at the 0–0 band of the fluorescence, goes from positive to negative as the proposed first and second transitions of IBB and AC are excited.[26] This result parallels that for C, where the first and second transitions are clearly separated in the spectrum.[27]

For the present series of amines the various absorption parameters (*cf.* Table I) are quite similar with the exception of the oscillator strength f of the second transition. All valence electron calculations (CNDO–CI) provide some useful information in this connection.[28] They indicate that the increase in f can, at least in part, be attributed to an increase in the charge-transfer character of the corresponding transition as the molecule becomes increasingly nonplanar. Thus, the second transition in C is mainly localized in the benzene rings, while the same transition in DPA shows a large charge-transfer contribution.

The intersystem crossing rate constant (k_{isc}) and quantum yield (ϕ_{isc}), and the derived triplet state deactivation parameters given in Tables II and III, were calculated with the assumption that only fluorescence and intersystem crossing processes deactivate the lowest excited singlet states of the compounds. The neglect of the internal conversion process $S_1 \rightarrow S_0$ seems to be justified for DPA, IBB, and AC in EPA solvent at 77°K, because the total emission quantum yield, $\phi_f + \phi_p$, accounts for 83–89% of the absorbed light. Since the measured fluorescence lifetimes of these molecules are short (τ_f = 2–10 nsec), it is likely that internal conversion to the ground state cannot compete effectively with the other two processes. This means that nonradiative processes between the lowest triplet and the ground state contribute to deactivation. In DPA there is some evidence to suggest that part of the nonradiative deactivation from the lowest triplet state at 77°K is channeled into photochemistry.[29]

In carbazole, however, this assumption needs to be further examined. Here, only 68% of the absorbed quanta are reemitted in radiative processes in EPA solvent at 77°K, and the fluorescence lifetime is longer, τ_f = 15 nsec. By means of a cis–trans isomerization technique the intersystem crossing quantum yield was found to be $\phi_{isc} = 0.4$.[30] This datum, together with the fluorescence quantum yield, may mean that internal conversion from S_1 can account for about 15% of deactivation in C at room temperature. Since ϕ_f is not significantly temperature dependent, it is likely that internal conversion from S_1 is also temperature independent and may be responsible for *ca.* 15% deactivation at

(24) K. Kimura, H. Tsubomura, and S. Nagakura, *Bull. Chem. Soc. Jap.*, 37, 1336 (1964).
(25) Calculated from data in ref 22.
(26) (a) J. R. Huber and J. E. Adams, to be published; (b) see also J. E. Adams, Doctoral Thesis, Northeastern University, 1972.
(27) H. Schütt and H. Zimmermann, *Ber. Bunsenges. Phys. Chem.*, **67**, 54 (1963); S. C. Chakravorty and S. C. Ganguly, *J. Chem. Phys.*, **52**, 2760 (1970).
(28) J. R. Huber, to be published; see also ref 26b.
(29) E. W. Förster and K. H. Grellmann, *J. Amer. Chem. Soc.*, **94**, 634 (1972).
(30) A. A. Lamola and G. S. Hammond, *J. Chem. Phys.*, **43**, 2129 (1965).

77°K. If this be the case, k_{isc}, k_p^0, and k_{nr} would decrease to 2.7×10^7, 0.077, and 0.053 sec^{-1}, respectively. Changes of this order of magnitude would alter the relative deactivation efficiencies among the various channels only slightly, and would not affect the conclusion to be drawn from the results.

Several important trends in the emission properties of aromatic amines are immediately evident upon inspection of the experimental data in Tables II and III. The fluorescence quantum yields increase smoothly from DPA to C, and the ϕ_p/ϕ_f ratios decrease, indicating that the fluorescence deactivation pathway becomes progressively more efficient, while the intersystem crossing becomes less efficient, throughout the series. Likewise, the phosphorescence lifetimes are increasing. To put this behavior on a more quantitative basis, we now examine the rate constants which govern the relaxation processes of the excited state.

Comparison of the rate constants for the amines reveals a particularly striking fact: k_{isc} and k_p^0, the intersystem crossing rate constant and the radiative phosphorescence rate constant, respectively, decrease dramatically in going from DPA to C, while k_f^0, and k_{nr}, the radiative fluorescence rate constant and nonradiative triplet decay constant, respectively, change only slightly throughout the series. It appears, therefore, that k_{isc} and k_p^0 are parameters which are particularly sensitive to the molecular geometry since the crucial differences among the compounds pertain to their nuclear configurations. Both the radiative (phosphorescence) and radiationless intersystem crossing processes between the singlet and triplet manifolds are spin forbidden and are allowed only through the spin–orbit coupling of electronic motion in the presence of nuclear potential fields. We conclude, therefore, that the excited state behavior of aromatic amines is *dominated by the influence of molecular geometry on spin–orbit coupling.*

The relatively small changes in k_f^0 in the series DPA to C do not account for differences of an order of magnitude in the values of k_{isc}. This implies that the increase in the fluorescence efficiency from DPA to C is only the reflection of a gradually closing intersystem crossing channel.

Recently, the theoretical description of intersystem crossing processes (isc) has received much attention. In utilizing the results of theoretical studies by Siebrand, Henry, and coworkers[31] for aromatic amines, only the direct spin–orbit coupling (soc) matrix elements are considered, since these integrals should govern the isc if the transition is orbitally allowed. The isc rate constant can be related to this integral by

$$k_{isc} \propto |\langle {}^1\phi_n | H_{soc} | {}^3\phi_m \rangle|^2 |\langle \chi_n | \chi_m \rangle|^2$$

where H_{soc} is the soc operator for a fixed equilibrium configuration of the nuclei, ϕ_n and ϕ_m are the electronic wavefunctions of the interacting singlet and triplet states, respectively, and $\langle \chi_n | \chi_m \rangle$ is the vibrational overlap integral.

DPA which is considered to have C_2 symmetry (less likely C_s) allows direct spin–orbit coupling between any singlet and triplet state. Carbazole, on the other hand, is known to have C_{2v} symmetry,[32] which introduces symmetry restriction into soc. The most effective soc route in this molecule involves high lying $\sigma\pi^*$ and $\pi\sigma^*$ singlet states of B_2 character, since only such states can give rise to the observed out-of-plane polarization of the phosphorescence.

The geometries of IBB and AC are not experimentally known, but one can predict, on the basis of chemical intuition and the examination of molecular models, that AC is nearly planar and that IBB, which contains a seven-member ring, is bent in such a way that the phenyl rings are not coplanar. However, the similarity of the polarization spectra[26] of IBB, AC, and C indicate that the molecular orbitals of IBB and AC experience some C_{2v} symmetry.

Since the k_{isc} values vary smoothly from DPA, IBB, and AC to C, it is likely that the increasing planarity in the molecular geometry, which becomes evident by increasing C_{2v} character from DPA to C, is responsible to a considerable degree for the decrease in soc throughout this series. The transformation of molecular configuration from C_2 symmetry to C_{2v} imposes gradual constraints on some soc routes which are symmetry allowed for the former case and forbidden in the latter case.

Lim and Chakrabarti[4] have shown that intramolecular charge-transfer transitions play an important role in soc of aniline molecules. It is expected that transitions with charge-transfer character are important for the present amines, too. Indeed, calculations predict a general increase of charge-transfer character in singlet transitions in going from the planar C to the nonplanar DPA. As the amine molecule becomes increasingly nonplanar, the nonbonding character of the nitrogen lone pair electron is increasing. This behavior leads to an enhancement of soc by charge-transfer transitions, which is somehow similar to the enhancement of soc by $n \rightarrow \pi^*$ transitions in heteroaromatic molecules.[4]

It appears at this point that two properties are important for soc in aromatic amines: the molecular symmetry which restricts soc mechanisms, and the extent of charge-transfer character in the electronic transitions involved in soc. Both properties, however, are determined by the molecular geometry of the aromatic amine molecule.

Acknowledgments. Support of this research by a Frederick Gardner Cottrell Grant of the Research Corporation is acknowledged. We are very grateful to Professor A. Halpern, New York University, for allowing us to use his nanosecond fluorescence spectrometer, and for his advice in the data analysis. Thanks are also due to Professor K. Weiss and Mr. T. V. Morris for many helpful suggestions.

(31) B. R. Henry and W. Siebrand, *J. Chem. Phys.*, **54**, 1072 (1971); V. Lawetz, G. Orlandi, and W. Siebrand, *ibid.*, **56**, 4058 (1972).

(32) M. Kurahashi, M. Fukuyo, A. Shimada, A. Furusaki, and I. Nitta, *Bull. Chem. Soc. Jap.*, **39**, 2564 (1966).